Dalton Transactions

PAPER

View Article Online
View Journal | View Issue

Cite this: *Dalton Trans.*, 2015, **44**, 16127

A cyclometallated fluorenyl Ir(III) complex as a potential sensitiser for two-photon excited photodynamic therapy (2PE-PDT)†

Elizabeth M. Boreham,[a,b] Lucy Jones,[a,b] Adam N. Swinburne,[a,b] Mireille Blanchard-Desce,[c] Vincent Hugues,[c] Christine Terryn,[d] Fabien Miomandre,[e] Gilles Lemercier*[f,g] and Louise S. Natrajan*[a,b]

Received 17th May 2015,
Accepted 10th August 2015

DOI: 10.1039/c5dt01855b

www.rsc.org/dalton

A new Ir(III) cyclometallated complex bearing a fluorenyl 5-substituted-1,10-phenanthroline ligand ([Ir(ppy)$_2$(**L1**)][PF$_6$], ppy = 2-phenylpyridine) is presented which exhibits enhanced triplet oxygen sensing properties. The efficacy of this complex to act as a photosensitiser for altering the morphology of C6 Glioma cells that represent malignant nervous tumours has been evaluated. The increased heavy metal effect and related spin–orbit coupling parameters on the photophysical properties of this complex are evidenced by comparison with Ru(II) analogues. The complex [Ir(ppy)$_2$(**L1**)][PF$_6$] is shown to exhibit relatively high two-photon absorption efficiencies for the lowest energy MLCT electronic transitions with two-photon absorption cross sections that range from 50 to 80 Goeppert–Mayer units between 750 to 800 nm. Quantum yields for the complex were measured up to 23% and the Stern–Volmer quenching constant, K_{SV} was determined to be 40 bar^{-1} in acetonitrile solution, confirming the high efficiency of the complex as a triplet oxygen sensitiser. Preliminary *in vitro* experiments with C6 Glioma cells treated with [Ir(ppy)$_2$(**L1**)][PF$_6$], show that the complex is an efficient sensitizer for triplet oxygen, producing cytotoxic singlet oxygen ($^1O_2$) by two-photon excitation at 740 nm resulting in photodynamic effects that lead to localised cell damage and death.

Introduction

Cyclometalated Ir(III) complexes are robust, synthetically versatile and both photochemically and thermally stable. Ir(III) has also attracted attention as it facilitates very efficient inter-system crossing (ISC) due to its large spin–orbit coupling value, ultimately leading to quantitative population of the molecule's triplet excited state.[1] This long-lived triplet metal-to-ligand charge transfer excited state (^{3}MLCT) can be populated either directly or *via* energy redistribution from excited singlet states located on the surrounding organic ligands.[2] The spin-forbidden nature of the radiative decay process is slightly relaxed due to partial triplet character of the ground state,[2] resulting in high phosphorescence quantum efficiency from the lowest triplet excited state. This results in a large Stokes shift between excitation and emission and provides an efficient mechanism for triplet–triplet energy transfer (Förster mechanism) to the ground state of $^3O_2$, so generating cytotoxic $^1O_2$. Additionally, Ir(III) polypyridyl based complexes enable broader tuning of the intrinsic photophysical properties[3] when compared to the lighter group congeners Fe(II) and Ru(II). This is principally due to increased ligand-field stabilization energy and pronounced decoupling of the ^{3}MLCT excited states with those that are metal-centred; these are essentially thermally inaccessible under ambient conditions.[4] For instance, homoleptic Ir(III) complexes, such as the related compound Ir(ppy)$_3$ possess desirable spectroscopic properties including long-lived electronic emitting states and high photo-luminescence quantum

[a]*School of Chemistry, The University of Manchester, Oxford Road, Manchester, M13 9PL, UK. E-mail: louise.natrajan@manchester.ac.uk*
[b]*Photon Science Institute, The University of Manchester, Oxford Road, Manchester, M13 9PL, UK*
[c]*Institut des Sciences Moléculaires, CNRS CNRS 5255, Univ. de Bordeaux, 351 cours de la Libération, F-33405, France*
[d]*Plate-forme IBISA, SFR CAP-SANTE, Université de Reims Champagne-Ardenne, Reims, France*
[e]*Laboratoire PPSM, UMR CNRS 8531, Ecole Normale Supérieure de Cachan, 61 Avenue du Président Wilson, F-94235 Cachan, France*
[f]*University of Reims Champagne-Ardenne, Institut de Chimie Moléculaire de Reims UMR CNRS no 7312-C^{2}POM Team, Moulin de la Housse B.P. 1039, F-51687 Reims Cedex 2, France. E-mail: gilles.lemercier@univ-reims.fr*
[g]*GdR CNRS no 3049 "Photomed", France*

†Electronic supplementary information (ESI) available: Stern–Volmer analysis of **IrppyL1** with O_2, overlay of one photon and two photon emission spectra of **IrppyL1**, spectroelectrochemistry of **IrppyL1** and single crystal X-ray data in cif format of [Ir(ppy)2(**L1**)][PF6]. CCDC 1401349. For ESI and crystallographic data in CIF or other electronic format see DOI: 10.1039/c5dt01855b

efficiencies.[5] As with Ru(II) complexes, the kinetic inertness of the coordination sphere of most Ir(III) complexes permits the construction of heteroleptic complexes,[6] but also the use of dedicated complexes as synthons on which to graft additional functional organic chromophores (the concept of "chemistry on the complex"[7]). For these reasons homo- and heteroleptic Ir(III) complexes have been used extensively for sensing and bio-imaging,[8] for example as the light-emitting component in organic light-emitting devices,[9] and in triplet–triplet annihilation upconversion schemes.[10] The MLCT transitions occurring within such complexes have implicit long-range (donor–acceptor) charge transfer character, which is known to be crucial for enhanced nonlinear optical (NLO) properties, including two-photon absorption (2PA). In this context, certain cyclometallated Ir(III) complexes have been reported to be relatively good two photon absorbers, more than suitable for applications involving 2PA.[11] During the preparation of this manuscript, Zhao *et al.* reported the three-photon absorption of related cyclometallated Ir(III) complexes with oligofluorene substitution.[12]

Two photon absorption is a third order NLO phenomenon in which the simultaneous absorption of two photons occurs under high intensity laser irradiation (high photon flux, such as that delivered by short-pulse lasers) leading to population of electronic excited states usually accessed with visible or UV light. Additionally, due to the quadratic nature of 2PA, high spatial resolution of excitation is possible when using focused light since excitation only occurs in the focal volume of the femtosecond pulsed laser (around a femtolitre).

One of the biological applications that Ir(III) polypyridyl complexes are particularly suitable for is photodynamic therapy (PDT). PDT is a non-invasive clinical treatment for certain cancers, pre-cancerous lesions and other non-malignant illnesses including age-related macular degeneration and viral infections (amongst others). A photosensitiser (PS) with a predominant triplet excited state character is employed to generate cytotoxic $^1O_2$ in the area under irradiation, thereby locally destroying affected cells. By using two-photon excitation, it is possible to use light in the biologically more transparent near-IR (nIR) region, where tissue is less absorbing, leading to deeper penetration of light into biological tissue (typically ≥ 500 μm).[13] While the compound Photofrin® (porfimer sodium, a porphyrin oligomer), is the most commonly used commercial PS for visible one-photon PDT in patients with endobronchial non-small-cell lung cancer, related tetrapyrroles and conjugated porphyrin derivatives have enabled the development of more efficient one and two photon red and nIR photosensitsers (700–900 nm).[14] However, 2PA is often desirable for the localisation of irradiation area and minimisation of damage to healthy peripheral tissue. The 2PA cross-section of Photofrin® was evaluated to be around 7 GM (Goeppert–Mayer units, and 1 GM = 10^{-50} cm^4 s per molecule per photon) at 850 nm. Supra-molecular edifices based on prophyrins[15] can give very high 2PA cross section values of up to 7600 GM. Nevertheless, it is also important to maximise the $^1O_2$ generation efficiency, *via* variation and optimisation of the excited state characteristics of the PS.

We reported previously the interest of 5-substituted-1,10-phenathroline ligand-based Ru(II) complexes for their linear and nonlinear optical properties, and their potential application in optical power limiting[16] and as photosensitisers for 2PE-PDT.[17] The 5-fluorenyl-substituted-1,10-phenanthroline ligand, **L1** (see Fig. 1 for the molecular structure) was chosen for its distinctive optical properties and its ability to complex heavy transition metals. It has been shown that the two-photon absorption cross section (σ_2) of Ru(II) phenanthroline (phen) complexes is increased by coordination of the fluorene pendent at the fifth position of phen in $[Ru(phen)_2(\mathbf{L1})]^{2+}$ compared to the unsubstituted 1,10-phenanthroline ligand in $[Ru(phen)_3]^{2+}$ (from 20 to 40 GM at around 740 nm)[18] Additionally, the non-planar geometry of this ligand can prevent aggregation, which may limit aggregation induced self-quenching and exciplex formation at higher localised concentrations in addition to affecting the biological distribution of the compound in a as far as potential bio-applications are concerned. Control of the solubility of the complex is afforded by substitution of the alkyl chain *e.g.* with triethylene glycol (TEG) for water solubility, with no detrimental effect on the photophysical properties. Previously, a homoleptic Ru(II) complex with three coordinated **L1** ligands featuring the TEG functionality was reported as a fairly efficient photosensitiser proposed for two-photon PDT; a 2PA cross-section σ_{2PA} around 40 GM was determined at 740 nm which corresponds to the wavelength used in the two-photon biological experiments.[19]

In this work, a heteroleptic Ir(III) complex has been synthesised involving two cyclometallating 2-phenylpyridine (ppy) ligands and 5-fluorene-1,10-phenanthroline (**L1**) as the third ligand ($[Ir(ppy)_2(\mathbf{L1})][PF_6]$). This complex is assessed as a two-photon absorber, and for its potential as a triplet O_2 sensitizer; its effectiveness as a 2PE-PDT therapeutic agent is evaluated by preliminary *in vitro* tests with C6 Glioma cells.

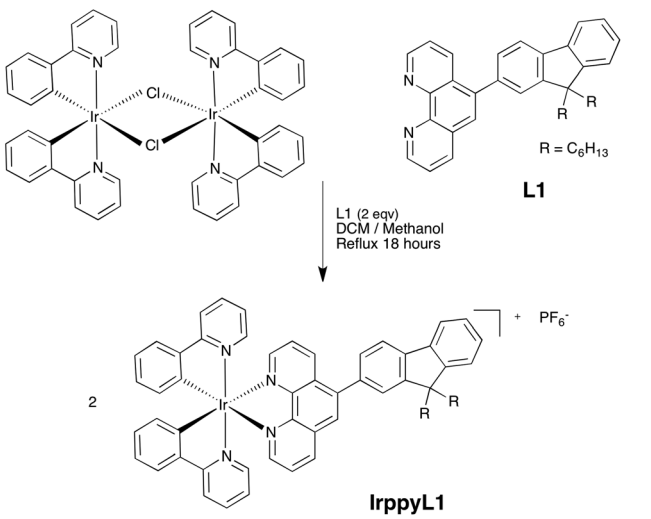

Fig. 1 Synthesis of $[Ir(ppy)_2(\mathbf{L1})][PF_6]$ (**IrppyL1**) from the chloro-bridged Ir(III) ppy dimer and ligand **L1** (R = C_6H_{13}).

Results and discussion

Synthesis

The complex $[Ir(ppy)_2(\mathbf{L1})][PF_6]$ (**IrppyL1**) was synthesised according to literature precedent from $[Ir(ppy)_2(\mu\text{-}Cl)]_2$ [20] by heating a dichloromethane : methanol solution of the dimer to reflux temperature with two equivalents of **L1**[18] (see Fig. 1). The complex was fully characterised by ^{1}H NMR, mass spectrometry, elemental analysis and singe crystal X-ray diffraction (see Experimental section).

Single crystals of **IrppyL1** for structural analysis were grown by slow vapour diffusion of *n*-hexanes into a dichloromethane : acetone solution of the complex at room temperature. In the solid state, the complex crystallises with two molecules of $[Ir(ppy)_2(\mathbf{L1})][PF_6]$ in the asymmetric unit cell. As expected, the PF_6^- counterions remain unbound to the metal centre. Each Ir(III) cation is hexacoordinated by two ppy ligands that lie in a mutually *cis* arrangement and one **L1** ligand providing an approximate octahedral coordination geometry about each Ir(III) ion (see Fig. 2). The average C–Ir and N–Ir bond lengths of 2.02(3) Å and 2.03(2) Å in the ppy ligands respectively and marginally longer N–Ir bond distances from the phen moiety of 2.112(15) Å are consistent with those reported in the literature for similar Ir(ppy)(phen) compounds. In the solid state, the dihedral angles between the fluorenyl substituent and the phen unit are measured as 48° in the molecule containing Ir(1) and 57° in the molecule labelled with Ir(2).

One-photon absorption and emission

The absorption spectrum of **IrppyL1** is composed of a broad, weak band in the 420–480 nm range attributed to triplet $d_{Ir(III)}$–π* metal-to-ligand charge-transfer (Fig. 3 and see ESI† for expanded graph). This is in accordance with previous assignments for this genre of Ir(III) complex involving ppy and polypyridyl ligands.[12,21] A broad and more intense band between 370 and 420 nm (λ_{max} around 400 nm), is assigned to the ^{1}MLCT, and finally bands at shorter wavelengths than 350 nm which are mainly ascribed to intra-ligand charge-transfer (ILCT) and π–π* electronic transitions centred on aromatic rings. These features are also reproduced in the excitation spectrum (see Fig. 3).

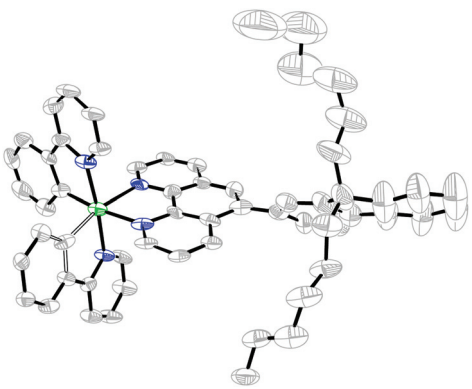

Fig. 2 Molecular structure of $[Ir(ppy)_2(\mathbf{L1})]PF_6$ with thermal ellipsoids set at the 50% probability level. H atoms, counterions and the second molecule in the asymmetric unit cell removed for clarity.

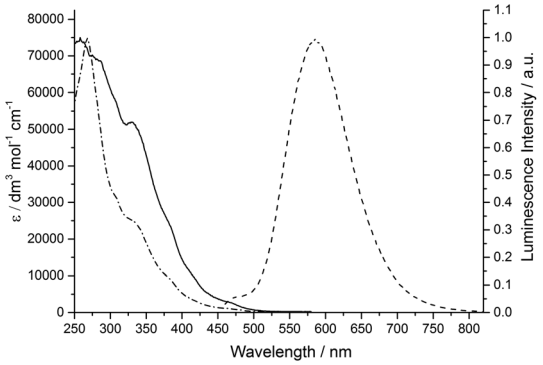

Fig. 3 Absorption (solid line), emission (dashed line) and excitation (dot-dashed line) spectra for **IrppyL1** in degassed acetonitrile at 2×10^{-5} M concentration (excitation at 400 nm, emission at 590 nm).

Table 1 Lifetimes and quantum yields for **IrppyL1** measured in acetonitrile solution at a concentration of 2×10^{-5} M and excitation wavelength of 400 nm (quantum yield error = ±3%)

Condition	τ/ns	Φ	k_r/s^{-1} ($\times 10^{-5}$)	k_{nr}/s^{-1} ($\times 10^{-5}$)
Degassed	748	0.23	2.7	9.1
In air	73	0.03	4.1	133.0
Oxygenated	19	0.01	3.7	525.0

The emission maximum wavelength is around 600 nm in acetonitrile. Given that the radiative decay-time of **IrppyL1** is of microsecond order, (see Table 1), the principal emissive excited state in the complex can be mainly ascribed as arising from the ^{3}MLCT state.

The absolute value of the quantum yield was measured at 400 nm excitation, in degassed acetonitrile using an integrating sphere and found to be 23% (see Table 1), the corresponding value in aerated and oxygenated solvent was found to be much lower (3 and 1%, respectively). In the solid state, the luminescence quantum yield was determined to be 40%.

Due to the envelope of absorption transitions at higher energy and the fact that the MLCT state is the principle constituent, the lowest energy absorption bands are best described as an admixture of ligand to ligand charge transfer (LLCT) and ligand-centred (LC) transitions. This is in agreement with the observed photophysics indicating the long range of the charge transfer transitions, as desired for nonlinear and especially two-photon absorption properties.

Computational study

In order to further elucidate the nature of the electronic transitions, density functional theory (DFT) calculations were per-

Table 2 First five singlet transitions: energies, oscillator strengths and orbital contributions for **IrppyL1** calculated by TDDFT

λ (nm)	f^a	Orbitals[b]	Description
402	0.0003	HOMO–LUMO (92%)	M^d/ppy(ph)–phen
354	0.0018	HOMO–LUMO+1 (90%)	M^d/ppy(ph)–phen
340	0.0917	HOMO–LUMO+2 (85%)	M^d/ppy(ph)–ppy(py)
339	0.3038	HOMO−1–LUMO (39%)	Fluorene–phen
		HOMO−1–LUMO+1 (22%)	Fluorene–phen
		HOMO−6–LUMO (15%)	M^d/ppy(ph)–phen
330	0.1634	HOMO−1–LUMO+1 (56%)	Fluorene–phen
		HOMO–LUMO+3 (11%)	M^d/ppy(ph)–phen
		HOMO−6–LUMO (9%)	M^d/ppy(ph)–phen

[a] f = oscillator strength of the transition. [b] Orbital percentage contributions.

formed on a simplified structure of the complex. The coordinates of the crystal structure were first altered to replace the hexyl chains with methyl groups for computational simplicity, as they do not contribute electronically. This structure was then optimised using DFT in Gaussian09[22] using the B3LYP functional and the 6-31G** basis set for C, H and N atoms and the Stuttgart relativistic basis set and effective core potential (ECP) for Ir.

The optimised structure was then used for time-dependent DFT (TDDFT) calculations with the same basis sets and the CAM-B3LYP functional, which describes charge-transfer transitions more accurately.[23] Table 2 lists the orbital contributions for the first singlet transitions, which support our assignments of the low energy, weak bands to MLCT transitions and the higher energy, more strongly absorbing bands to intra-ligand transitions, in particular from the fluorene pendant of **L1** to the phenanthroline moiety.

There are six triplet states calculated before the first singlet state, the lowest of these, T_1–S_0 is described as a mixture of MLCT from the Ir(III) d orbitals to the phen (30%) and intra-ligand transitions located on **L1** (50%) the remainder is made up of many smaller contributions.

Electrochemistry

In order to examine the effect of the charge transfer electronic transitions in the complex, the redox potential of Ir(III) in **IrppyL1** and the electrochemical properties of the system were investigated. One reversible, one-electron oxidation with the halfway redox potential at 0.87 V (*vs.* Fc^+/Fc) was observed for **IrppyL1** by cyclic voltammetry (C.V.) (see Fig. 4), characteristic of the oxidation of Ir(III) to Ir(IV).

This experiment was conducted in a classical cell at 1 mM concentration in acetonitrile with tetraethylamonium hexafluorophosphate as the electrolyte. In addition, the redox potential was also measured in a tailored spectro-electrochemical cell, which allows monitoring of the emission intensity upon an electrochemical signal. The emission can be partially switched off by oxidation of the metal from Ir(III) to Ir(IV) as shown in Fig. 5. This shows that the removed electron is

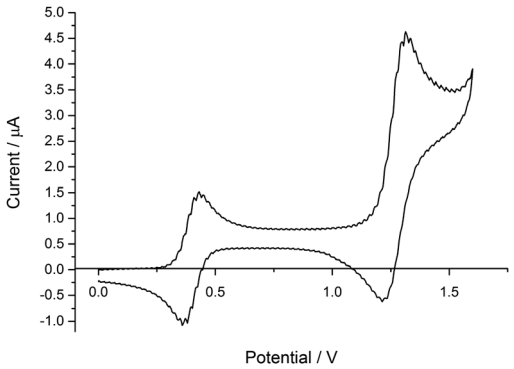

Fig. 4 Cyclic voltammogram of **IrppyL1** *vs.* Fc^+/Fc in acetonitrile (1 mM) degassed with N_2, measured at a scan rate of 50 mV s^{-1} showing one reversible oxidation at 0.87 V.

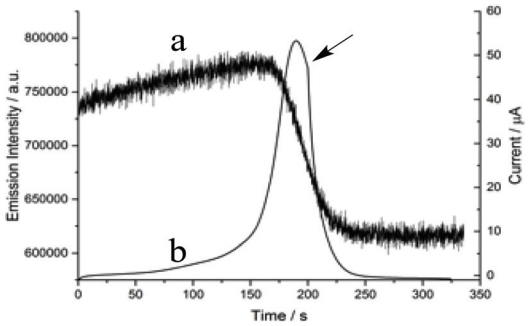

Fig. 5 Emission intensity (a) and electrochemical current (b) traces for **IrppyL1** (1 mM in acetonitrile with NEt_4PF_6 electrolyte) as a function of time upon linear potential sweep (5 mV s^{-1}). The arrow shows the time corresponding to the potential reversal.

responsible for the emissive transition and supports the assignment of MLCT character for this transition. Unfortunately it has not been possible to restore the luminescence upon re-reduction, possibly because of oxygen production at the counter electrode acting as a quencher.

Stern–Volmer studies

Since ground state (triplet) oxygen is a very efficient dynamic or collisional quencher of triplet excited states in platinum group complexes, Stern–Volmer analysis can provide a measure of the efficiency of this quenching process in terms of the quenching constant K_{SV}. In this regard, the potential of **IrppyL1** to act as a triplet oxygen sensitiser, was assessed by determining both the emission intensity and phosphorescent lifetime in degassed, air equilibrated and oxygen-saturated acetonitrile solutions The resulting relative lifetimes (τ_0/τ) and intensities (I_0/I) were then determined and plotted against the partial pressure of oxygen in solution to give the slope as K_{SV}, the Stern–Volmer quenching constant of triplet O_2 in this system (see Fig. 6).

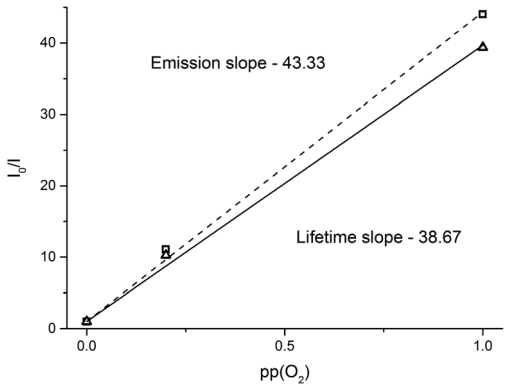

Fig. 6 Stern–Volmer plot of the relative emission intensities (squares) and lifetimes (triangles) against the partial pressure of oxygen in solution. Estimated error in I/I_0 based on 3 repeat measurements = ±2%, calculated lifetime error <±1% in all measurements and R^2 = 0.99 for both plots.

In fluid solution, the dependence of emission intensity and lifetime with quencher concentration is given by the Stern–Volmer equation (eqn (1)):

$$\frac{\tau_0}{\tau} = \frac{I_0}{I} = 1 + K_{SV}[O_2] = 1 + k_q\tau_0[O_2] = 1 + k_q\tau_0 K_H^{solv} P_{O_2} \quad (1)$$

where the I_s parameters are emission intensities, the τ_s are lifetimes, K_{SV} is the Stern–Volmer quenching constant, k_q is the bimolecular rate constant for quenching of the excited state, and, K_H^{solv}, the Henry constant of O_2 (gas) in a given solvent. The susbcript 0 denotes the values of the quantity in the absence of the quencher. Plots of I_0/I and τ_0/τ *vs.* oxygen concentration will be linear with identical slopes equal to K_{SV} if there is a single class of luminophores that are all equally accessible to the quencher. This is what is observed in the case of **IrppyL1** for both I_0/I and τ_0/τ representations. The gradient of the correlation line was determined to be 43 and 39 bar^{-1} for the emission intensity and radiative lifetime respectively. The similar values obtained in terms of both emission intensity and lifetime value are consistent with the mechanism proposed for this energy transfer and oxygen sensitizing. Interestingly, the values of K_{SV} are significantly higher in **IrppyL1** than in the analogous tris-phenanthroline derived ruthenium(II) complexes that we studied recently, where for example, the value of 5 was found for K_{SV} of complex $[(phen)_2Ru(phenCOOH)]^{2+}$ in water.[24]

The elevated Stern–Volmer constant for triplet oxygen quenching in **IrppyL1** when compared to that of unsubstituted Ru(II) based 1,10-phenanthroline complexes may arise from a higher phosphorescence quantum yield of the cyclometallated Ir(III) centre (Φ_{phos} = 23% *cf.* 9% for $[Ru(\mathbf{L1})_3]^{2+}$)[19] and the relaxed spin-forbidden transition caused by increased SOC. When the rate constants for radiative and non-radiative decay are considered alongside pO_2 (k_r and k_{nr}, see Table 1), k_r is similar for **IrppyL1** in all three solutions (around 3–4 × 10^5 s^{-1}) whereas k_{nr} is an order of magnitude greater in the aerated solution compared to the degassed solution, and higher again in the oxygen saturated (9.1, 133 and 525 × 10^5 s^{-1}, respectively) thereby confirming the presence of fast non-radiative relaxation pathways in the presence of oxygen. We were unable to measure the singlet oxygen quantum yield for **IrppyL1**, but for comparison, the experimentally measured values for the closely related systems [Ir(ppy)$_2$(bipy)] and [Ir(ppy)$_2$(phen)] are 0.97 and 0.93 respectively.[25]

Two-photon absorption studies

The emission profile of **IrppyL1** was shown to be identical to the one photon emission profile following non-resonant two-photon excitation with 150 fs nIR laser pulses (700–1000 nm), indicating that the same excited state is accessed by either method as anticipated (see ESI†). This inference is corroborated by the fact that the two-photon excitation spectrum at half the wavelength is superimposable upon the one photon excitation spectrum. The occurrence of a two-photon nonlinear process was further confirmed by power dependence measurements that showed a quadratic relationship of the two-photon induced emission intensity on laser power; this method has been described previously. The 2PA cross section was determined with reference to fluorescein in 0.01 M NaOH, for which σ_2 is well known.[13] The complex **Ir(ppy)$_2$L1** exhibits a 2PA cross-section (σ_2) of around 10 GM over a broad excitation range (800–1000 nm) due to non-resonant absorption populating the intra-ligand excited states in addition to the MLCT. Due to an increase in the IL character at shorter wavelengths, (supported by TDDFT) the σ_2 value then increases from 10 to 80 GM between 700 and 800 nm. These values are comparable to those obtained for the analogous Ru(II) complex [Ru(phen)$_2$**L1**][PF$_6$]$_2$ (10 GM at 900 nm, and 50 GM at 750 nm).[26] It is remarkable that the very weak resonant absorption band attributed to the ^{3}MLCT is relatively large by two-photon process (same average value for the 2PA cross-section at 960 and 800 nm, see Fig. 7); the symmetry and/or spin characteristics of this transition may well lie at the origin of this observation.

In vitro experiments

In preliminary *in vitro* experiments, confocal microscopy was used to evaluate C6 Glioma cell damage induced by photodynamic effects in the presence of **IrppyL1** under two-photon irradiation. The cell morphology is observed to change from an elongated (fibroblast) shape to round when they become unhealthy. C6 cells are a model of Glioma which represent a type of malignant tumour that originate in the brain, spine and nervous system. They may be considered to be the cause of aggressive primary brain tumours, which renders both C6 and Glioma cells attractive targets for PDT.

As a control experiment, a sample of cells in the absence of **IrppyL1**, was irradiated at 740 nm (32.5 μW) for 5 minutes (which corresponds to two cycles of irradiation). After this time, there was limited damage to the cells and only 7% of the total number of cells underwent a change in morphology.

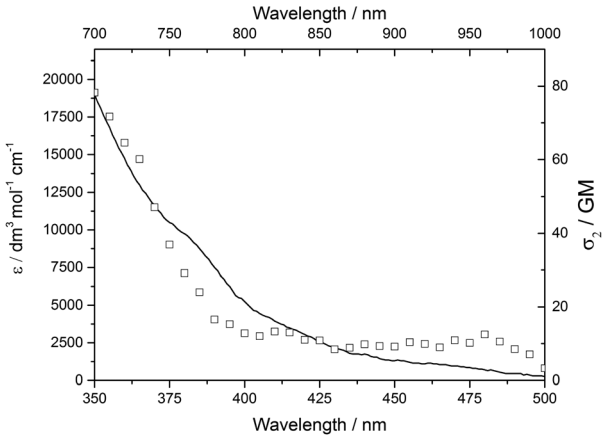

Fig. 7 Two-photon excitation (marked squares) and linear excitation (solid line) spectra of **IrppyL1** in degassed acetonitrile. (One-photon at 2×10^{-5} M, two-photon measurement at a concentration of 4×10^{-5} M, measured by two photon excited fluorescence (2PEF) referenced to fluorescein in 0.01 M NaOH, 1×10^{-4} M).

Therefore, it can be concluded that irradiation alone does not adversely affect the cells (Fig. 8).

The complex **IrppyL1** was then dissolved in 1% dimethyl sulphoxide and taken up in water to give concentrations of 10 μM and 1 μM. Cell samples were treated with the complex at each concentration before immediately undergoing two cycles of irradiation analogously to the Ir-untreated cells. At the higher concentration of 10 μM, 55% of the cells in the irradiated volume showed drastic modifications of the cellular morphology, while at the lower 1 μM concentration, 31% of the cells were affected. It was thus observed that the presence of both **IrppyL1** and light is required to cause significant damage to the cells and that the lower concentration of the complex (1 μM) is sufficient to cause substantial cell damage following two-photon irradiation at 740 nm.

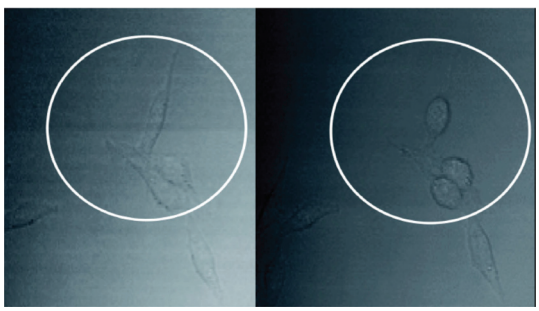

Fig. 8 Cells treated with 1 mM **IrppyL1** before (left) and after (right) 5 minutes irradiation (one such irradiation area of the whole sample irradiated is in the white circle) at 740 nm, 32.5 μW during 6 cycles) and 15 minutes wait – the morphology of the cells on the right has become rounded compared to the elongated shape of the healthy cells. Spot area = 0.13 μm which equates to an area of 0.0169 μm^2. The irradiation time per cycle = 50 s, the total light dose per pixel (1.91×10^{-4} s duration) = 3.72×10^{-8} J, which equates to 220 J cm^{-2}.

Conclusions

A new Ir(III) cyclometallated complex bearing the fluorene-phenanthroline ligand (**L1**) has been synthesised and fully characterised. The complex **IrppyL1** has a phosphorescent lifetime of 748 ns and a quantum yield of 23% in oxygen free solution, which are dramatically decreased in the presence of $^3O_2$. The triplet–triplet energy transfer process is extremely efficient with a Stern–Volmer quenching constant, K_{SV} of 40 bar^{-1} in solution. The 2PA cross-section, σ_2 at 740 nm was determined to be 45 GM. These values make the complex a good candidate for a 2PE-PDT photosensitiser and *in vitro* studies with C6 Glioma cells showed efficient cell damage where cells were treated with **IrppyL1** and irradiated under two-photon conditions with 740 nm fs pulsed light, while cells irradiated with no complex were unchanged. The change in morphology of the cells observed may be an indication that additional photodynamic cellular responses are occurring resulting from the presence of **IrppyL1** and we are currently investigating the mechanism(s) of cell damage in the presence of this and related photosensitisers. In addition to as (two-photon induced)-photodynamic therapy, due to the high efficiency of luminescence quenching in the presence of oxygen, the complex could also be utilised for oxygen sensing in other applications.[27]

Experimental section

General

Acetonitrile was dried over CaH_2 and distilled prior to use. All other chemicals were obtained from Sigma Aldrich and used as supplied. All air sensitive manipulations were conducted in an Ar filled glove box (Innovative Technologies PE2) total O_2 and H_2O content was always below 0.1 ppm. All NMR spectra were recorded on a Bruker Avance 400 spectrometer, operating frequency 400 MHz (^1H) and 136 Hz (^{13}C). Mass spectra were obtained using MALDI from methanol solutions with an ALPHA maxtrix on a Micromass TOF Spec 2E spectrometer. Elemental Analyses were performed by the microanalytical services at the University of Manchester using a Carlo ERBA Instruments CHNS-O EA1108 elemental analyzer (C, H and N analysis) and a Fisons Horizon elemental analysis ICP-OED spectrometer for P.

X-ray diffraction data for **IrppyL1** were collected at 100 K with a Bruker APEX 2 diffractometer using graphite-monochromated Mo-Kα radiation. The structure was solved by direct methods and refined using OLEX-2 software.[28] The structure was completed by iterative cycles of Δ*F*-syntheses and a full matrix least squares refinement. All non-H atoms were refined anisotropically and difference Fourier syntheses were employed in positioning idealised hydrogen atoms and were allowed to ride on their parent C or N-atoms. All refinements were against F^2 and used OLEX-2.

Synthesis of [Ir(ppy)$_2$L1][PF$_6$]

[Ir(ppy)$_2$(μ-Cl)]$_2$ (149 mg, 0.139 mmol) was dissolved in methanol (20 mL). This solution was added slowly to a solution of **L1** (150 mg, 0.293 mmol) in dichloromethane (15 mL). The resulting mixture was refluxed for 18 h. The solution was cooled to room temperature and a methanolic solution of ammonium hexafluorophospate (5 mL) was added. The solution was stirred for a further 30 min. The solvent was reduced to half volume and the precipitate filtered, washed with methanol (10 mL) and ether (10 mL) and dried to give orange crystals (243.3 mg, 75%). MALDI MS (alpha): m/z 1014 $\{M - PF_6\}^+$ (100%). ^{1}H NMR (400 MHz, d$_2$-DCM) δ_H: 8.62 (ddd $^3J_{HH}$ = 8.3 Hz, $^4J_{HH}$ = 1.4 Hz, 2H, phen), 8.37 (ddd $^3J_{HH}$ = 5.1 Hz, $^4J_{HH}$ = 4.1 Hz, 2H, phen), 8.23 (s, 1H, phen), 8.01 (m, 3H, fluorenyl), 7.84 (m, 7H, 2 phen, 4 ppy ph, 1 fluorenyl), 7.62 (m, 2H, fluorenyl), 7.46 (m, 5H, 2 ppy ph, 2 ppy py, 1 fluorenyl), 7.17 (tdd, $^3J_{HH}$ = 7.5 Hz, $^3J_{HH}$ = 3.5 Hz, $^4J_{HH}$ = 1.1 Hz, 2H, ppy py), 7.05 (tt, $^3J_{HH}$ = 7.5 Hz, $^4J_{HH}$ = 1.4 Hz, 2H, ppy py), 6.95 (td, $^3J_{HH}$ = 6.1 Hz, $^4J_{HH}$ = 1.1 Hz, 2H, ppy ph), 6.49 (ddd, $^3J_{HH}$ = 7.6 Hz, $^4J_{HH}$ = 2.7 Hz, $^4J_{HH}$ = 0.9 Hz, 2H, ppy py), 2.08 (m, 4H), 1.1 (m, 12H) 0.79 (m, 10H); ^{13}C NMR (136 Hz, $CDCl_3$) δ_C: 14.61 (CH_3), 23.35 (CH_2), 24.72 (CH_2), 30.44 (CH_2), 32.34 (CH_2), 41.02 (CH_2), 56.23 (q), 120.72 (CH), 120.96 (CH), 121.04 (CH), 123.70 (CH), 123.97 (CH), 124.07 (CH), 125.30 (CH), 125.79 (CH) 127.10 (CH), 127.87 (CH), 128.71 (CH), 129.65 (CH), 131.59 (CH), 131.81 (q), 132.63 (CH), 135.74 (q) 137.95 (CH), 139.10 (CH), 140.93 (q), 142.70 (q), 143.07 (q), 144.70 (q), 146.94 (q), 148.16 (q), 149.45 (CH), 150.09 (q), 150.49 (q), 151.84 (CH), 152.57 (q), 154.97 (q), 168.68 (q). UV-vis (acetonitrile) λ_{max}/nm (ε = mol^{-1} dm^3 cm^{-1}) 270 (74 800), 300 (sh) (32 900), 330 (sh) (25 000), 380 (sh) (9600). Anal. Calcd For $C_{59}H_{56}IrN_4PF_6$: C 61.18 H 4.89 N 4.84 P 2.67. Found C 61.06 H 4.97 N 4.80 P 2.44.

Photophysical characterisation

UV-visible spectra were recorded on a Shimadzu UV-2600 spectrometer using quartz cuvettes with a path length of 1 cm. Steady state emission spectra were recorded in quartz cuvettes on an Edinburgh Instrument FP920 Phosphorescence Lifetime Spectrometer equipped with a 5 W microsecond pulsed xenon flashlamp (with single 300 mm focal length excitation and emission monochromators in Czerny Turner configuration) and a red sensitive photomultiplier in peltier (air cooled) housing, (Hamamatsu R928P). Lifetime data were recorded following excitation with EPL 405 picosecond pulsed diode laser (Edinburgh Instruments) using time correlated single photon counting (PCS900 plug-in PC card for fast photon counting). Lifetimes were obtained by tail fit on the data obtained and quality of fit judged by minimization of reduced chi-squared. Absolute quantum yields were measured using an integration sphere (Edinburgh Instruments).

Stern–Volmer analysis

A dry degassed acetonitrile solution of **IrppyL1** was prepared in a glove box in a quartz cell equipped with a Young's tap (10 mm × 10 mm) for the oxygen free measurements. This solution was left open to equilibrate with the air for 1 hour to obtain an aerated sample and then bubbled with oxygen for 5 minutes to obtain an oxygen-saturated solution.

Electrochemistry

Measurements were performed on N_2 degassed acetonitrile solutions of 1 mM concentration, and tetrabutylammonium hexafluoro phosphate was used as the electrolyte salt. Cyclic voltammetry was performed in a three-electrode cell with a potentiostat (Versa-STAT4, Princeton Applied Research) driven by a PC. Platinum disk was used as the working electrode, with platinum wire as the counter and Ag wire as the reference electrode.

Electrochemical monitoring of the luminescence was performed in a tailored thin layer spectroelectrochemical cell coupled to a Fluorolog 3 (Horiba) spectrofluorimeter through optical fibers and driven by a CHI-600 potentiostat.[29]

In vitro cell experiments

Two-photon microscopy. C6 glioma cells were seeded at a density of 5 × 10^3 cells per well in 96-well plates and grown in Dulbecco's Modified Eagle Medium F12, enriched with 10% fetal calf serum (FCS) and antibiotics (penicillin 50 U ml^{-1}, streptomycin 50 mg ml^{-1}). After 24 h, cells were treated with **IrppyL1** at concentrations of 1 mM and 10 mM. A laser-scanning microscope LSM 710 NLO Zeiss (Iena, Germany) was used. Excitation was provided by a CHAMELEON femtosecond Titanium-Sapphire laser (Coherent, Santa Clara, USA) set at 740 nm with a photon flux of 0.025 mW cm^{-2}. Living cells were deposited in glass bottom box and were imaged with a 63 × 1.4 NA oil objective lens. The pathology of these cells is not affected by the presence of small quantities of DMSO.

Nonlinear optical measurements

The two-photon absorption spectra of the **Ir(ppy)$_2$L1** complex was determined in the 700–1000 nm range by investigating its two-photon excited luminescence (2PEL) in deoxygenated 10^{-4} mol L^{-1} acetonitrile solution in a 10 mm × 10 mm quartz cuvette. The measurements were performed using a Nd:YLF-pumped Ti:sapphire oscillator generating 150 fs pulses at a rate of 76 MHz. The excitation was focused into the cuvette through a microscope objective (10×, NA 0.25). The luminescence was detected in epifluorescence mode *via* a dichroic mirror (Chroma 675dcxru) and a barrier filter (Chroma e650sp-2p) by a compact CCD spectrometer module, BWTek BTC112E. Total luminescence intensities were obtained by integrating the corrected emission spectra measured by this spectrometer. 2PA cross-sections (σ_2) were determined from the two-photon excited luminescence cross-sections ($\sigma_2\Phi$) and the luminescence emission quantum yield (Φ). 2PEL cross-sections of 10^{-4} M solutions were measured relative to a 10^{-4} M solution of fluorescein in 0.01 M aqueous NaOH for the range 700–1000 nm, using the well-established method described by Xu and Webb[13] and the appropriate solvent-related refractive index corrections.[30] Data points between 700 and 715 nm were corrected.[31] The quadratic dependence of the luminescence

intensity on the excitation power was checked for each sample at all wavelengths, indicating that the measurements were carried out in intensity regimes where saturation or photodegradation did not occur.

Acknowledgements

The authors thank S. Dukic and L. van Gulick for cell preparations. GL thanks ANR P2N PDTX for funding: "Région Champagne-Ardenne" and Europe (FEDER) for the financial support (laser scanning microscope LSM). MBD thanks Conseil General d'Aquitaine for funding ("Chaire d'accueil" grant and fellowship to VH). LSN thanks Simon Randall and Daniel Whittaker for help with X-ray crystallography, the EPSRC for a studentship for EMB and LJ and for a Career Acceleration Fellowship for LSN and The University of Manchester for financial support.

Notes and references

1 F. N. Castellano, I. E. Pomestchenko, E. Shikhova, F. Hua, M. L. Muro and N. Rajapakse, *Coord. Chem. Rev.*, 2006, **250**, 1819.
2 F. Spaenig, J.-H. Olivier, V. Prusakova, P. Retailleau, R. Ziessel and F. N. Castellano, *Inorg. Chem.*, 2011, **50**, 10859.
3 M. A. Baldo, M. E. Thompson and S. R. Forrest, *Nature*, 2000, **403**(6771), 750.
4 J. B. Waern, C. Desmarets, L.-M. Chamoreau, H. Amouri, A. Barbieri, C. Sabatini, B. Ventura and F. Barigelletti, *Inorg. Chem.*, 2008, **47**, 3340.
5 M. S. Lowry and S. Bernhard, *Chem. – Eur. J.*, 2006, **12**, 7970.
6 I. M. Dixon, J.-P. Collin, J.-P. Sauvage and L. Flamigni, *Inorg. Chem.*, 2001, **40**, 5507.
7 A. A. Rachford, R. Ziessel, T. Bura, P. Retailleau and F. N. Castellano, *Inorg. Chem.*, 2010, **49**, 3730; C. Goze, D. V. Kozlov, F. N. Castellano, J. Suffert and R. Ziessel, *Tetrahedron Lett.*, 2003, **44**, 8713.
8 Q. Zhao, C. Huang and F. Li, *Chem. Soc. Rev.*, 2011, **40**, 2508.
9 S. Lamansky, P. Djurovich, D. Murphy, F. Abdel-Razzaq, H.-E. Lee, C. Adachi, P. E. Burrows, S. R. Forrest and M. E. Thompson, *J. Am. Chem. Soc.*, 2001, **123**, 4304; C.-H. Yang, J. Beltran, V. Lemaur, J. Cornil, D. Hartmann, W. Sarfert, R. Froeohlich, C. Bizzarri and L. De Cola, *Inorg. Chem.*, 2010, **49**, 9891; H.-S. Duan, P.-T. Chou, C.-C. Hsu, J.-Y. Hung and Y. Chi, *Inorg. Chem.*, 2009, **48**, 6501; E. A. Plummer, V. A. Dijken, H. W. Hofstraat, L. D. Cola and K. Brunner, *Adv. Funct. Mater.*, 2005, **15**, 281.
10 W. Zhao and F. N. Castellano, *J. Phys. Chem. A*, 2006, **110**, 11440.
11 R. M. Edkins, S. L. Bettington, A. E. Goeta and A. Beeby, *Dalton Trans.*, 2011, **40**, 12765–12770.
12 Y. Fan, D. Ding and D. Zhao, *Chem. Commun.*, 2015, **51**, 3446–3449.
13 C. Xu and W. W. Webb, *J. Opt. Soc. Am. B*, 1996, **13**, 481.
14 A. Karotki, M. Khurana, J. R. Lepock and B. C. Wilson, *Photochem. Photobiol.*, 2006, **82**, 443; E. Dahlstedt, H. A. Collins, M. Balaz, M. K. Kuimova, M. Khurana, B. C. Wilson, D. Phillips and H. L. Anderson, *Org. Biomol. Chem.*, 2009, **7**, 897.
15 K. Ogawa, A. Ohashi, Y. Kobuke, K. Kamada and K. Ohta, *J. Am. Chem. Soc.*, 2003, **125**, 13356.
16 M. Four, D. Riehl, O. Mongin, M. Blanchard-Desce, L. M. Lawson-Daku, J. Moreau, J. Chauvin, J. A. Delaire and G. Lemercier, *Phys. Chem. Chem. Phys.*, 2011, **13**, 17304; C. Girardot, B. Cao, J.-C. Mulatier, P. L. Baldeck, J. Chauvin, D. Riehl, J. A. Delaire, C. Andraud and G. Lemercier, *ChemPhysChem*, 2008, **9**, 1531.
17 G. Boeuf, G. V. Roullin, J. Moreau, L. Van Gulick, N. Zambrano Pineda, C. Terryn, D. Ploton, M.-C. Andry, F. Chuburu, S. Dukic, M. Molinari and G. Lemercier, *ChemPlusChem*, 2014, **79**, 171.
18 C. Girardot, G. Lemercier, J.-C. Mulatier, J. Chauvin, P. L. Baldeck and C. Andraud, *Dalton Trans.*, 2007, 3421.
19 C. Boca, M. Four, A. Bonne, B. van Der Sanden, S. Astilean, P. L. Baldeck and G. Lemercier, *Chem. Commun.*, 2009, 4590.
20 S. Sprouse, K. A. King, P. J. Spellane and R. J. Watts, *J. Am. Chem. Soc.*, 1984, **106**, 6647.
21 S. Lamansky, P. Djurovich, D. Murphy, F. Abdel-Razzaq, R. Kwong, I. Tsyba, M. Bortz, B. Mui, R. Bau and M. E. Thompson, *Inorg. Chem.*, 2001, **40**, 1704.
22 M. J. Frisch, G. W. Trucks, H. B. Schlegel, G. E. Scuseria, M. A. Robb, J. R. Cheeseman, G. Scalmani, V. Barone, B. Mennucci, G. A. Petersson, H. Nakatsuji, M. Caricato, X. Li, H. P. Hratchian, A. F. Izmaylov, J. Bloino, G. Zheng, J. L. Sonnenberg, M. Hada, M. Ehara, K. Toyota, R. Fukuda, J. Hasegawa, M. Ishida, T. Nakajima, Y. Honda, O. Kitao, H. Nakai, T. Vreven, J. A. Montgomery Jr., J. E. Peralta, F. Ogliaro, M. Bearpark, J. J. Heyd, E. Brothers, K. N. Kudin, V. N. Staroverov, R. Kobayashi, J. Normand, K. Raghavachari, A. Rendell, J. C. Burant, S. S. Iyengar, J. Tomasi, M. Cossi, N. Rega, J. M. Millam, M. Klene, J. E. Knox, J. B. Cross, V. Bakken, C. Adamo, J. Jaramillo, R. Gomperts, R. E. Stratmann, O. Yazyev, A. J. Austin, R. Cammi, C. Pomelli, J. W. Ochterski, R. L. Martin, K. Morokuma, V. G. Zakrzewski, G. A. Voth, P. Salvador, J. J. Dannenberg, S. Dapprich, A. D. Daniels, Ö. Farkas, J. B. Foresman, J. V. Ortiz, J. Cioslowski and D. J. Fox, *GAUSSIAN 09 (Revision D.01)*, Gaussian, Inc., Wallingford CT, 2009.
23 M. J. G. Peach, P. Benfield, T. Helgaker and D. J. Tozer, *J. Chem. Phys.*, 2008, **128**, 044118.
24 C. Truillet, F. Lux, J. Moreau, M. Four, L. Sancey, S. Chevreux, G. Boeuf, P. Perriat, C. Frochot, R. Antoine, P. Dugourd, C. Portefaix, C. Hoeffel, M. Barberi-Heyob, C. Terryn, L. van Gulick, G. Lemercier and O. Tillement, *Dalton Trans.*, 2013, **42**, 12410.

25 S.-Y. Takizawa, R. Aboshi and S. Murata, *Photochem., Photobiol.*, 2011, **10**, 895.
26 G. Lemercier and M. Blanchard-Desce, unpublished results, 2015.
27 S. Sakadžić, E. Roussakis, M. A. Yaseen, E. T. Mandeville, V. J. Srinivasan, K. Arai, S. Ruvinskaya, A. Devor, E. H. Lo, S. A. Vinogradov and D. A. Boas, *Nat. Methods*, 2010, **7**, 755.
28 O. V. Dolomanov, L. J. Bourhis, R. J. Gildea, J. A. K. Howard and H. Puschmann, A complete structure solution, refinement and analysis program (2009), *J. Appl. Crystallogr.*, 2009, **42**, 339.
29 C. Quinton, V. Alain-Rizzo, C. Dumas, F. Miomandre, G. Clavier and P. Audebert, *Chem. – Eur. J.*, 2015, **21**, 2230.
30 M. H. V. Werts, N. Nerambourg, D. Pélégry, Y. Le Grand and M. Blanchard-Desce, *Photochem. Photobiol. Sci.*, 2005, **4**, 531.
31 C. Katan, S. Tretiak, M. H. V. Werts, A. J. Bain, R. J. Marsh, N. Leonczek, N. Nicolaou, E. Badaeva, O. Mongin and M. Blanchard-Desce, *J. Phys. Chem. B*, 2007, **111**, 9468.